Phase I Trial of the Antivascular Agent Combretastatin A4 Phosphate on a 5-Day Schedule to Patients With Cancer: Magnetic Resonance Imaging Evidence for Altered Tumor Blood Flow

By James P. Stevenson, Mark Rosen, Weijing Sun, Maryann Gallagher, Daniel G. Haller, David Vaughn, Bruce Giantonio, Ross Zimmer, William P. Petros, Michael Stratford, David Chaplin, Scott L. Young, Mitchell Schnall, and Peter J. O'Dwyer

Purpose: **Combretastatin A4 (CA4) phosphate (CA4P) inhibits microtubule polymerization and is toxic to proliferating endothelial cells in vitro. It causes reversible vascular shutdown in established tumors in vivo, consistent with an antivascular mechanism of action. The present study investigated escalating doses of CA4P administered intravenously to patients with advanced cancer.**

Patients and Methods: **Patients with solid malignancies and good performance status received CA4P as a 10-minute infusion daily for 5 days repeated every 3 weeks. Pharmacokinetic sampling was performed during cycle 1. Patients receiving ≥ 52 mg/m²/d had serial dynamic contrast-enhanced magnetic resonance imaging (DCE-MRI) studies to measure changes in tumor perfusion with CA4P treatment.**

Results: **Thirty-seven patients received 133 treatment cycles. CA4P dose levels ranged from 6 mg/m² to 75 mg/m² daily. Severe pain at sites of known tumor was dose limiting at 75 mg/m². Dose-limiting cardiopulmonary toxicity (syncope and dyspnea or hypoxia) was noted as well in two patients treated at 75 mg/m². Other toxicities included hypotension, ataxia, dyspnea, nausea or vomiting, headache, and transient sensory neuropathy. Plasma CA4P and CA4 area under the concentration-time curve and maximal concentration values increased linearly with dose. Tumor perfusion, as measured by the first-order rate constant of gadolinium plasma to tissue transfer during DCE-MRI studies, was found to decrease in eight of 10 patients. Relationships were also demonstrated between perfusion changes and pharmacokinetic indices. A partial response was observed in a patient with metastatic soft tissue sarcoma, and 14 patients exhibited disease stability for a minimum of two cycles.**

Conclusion: **Doses of CA4P on a daily times five schedule of 52 to 65 mg/m² were reasonably well-tolerated. The 52 mg/m² dose is recommended for further study based on cumulative phase I experience with CA4P. Antitumor efficacy was observed, and the use of DCE-MRI provided a valuable noninvasive measure of the vascular effects of CA4P treatment.**

J Clin Oncol 21:4428-4438. *© 2003 by American Society of Clinical Oncology.*

BLOOD VESSELS that make up tumor neovasculature are necessary for the growth and survival of established malignancy.[1] The destruction of nascent tumor vasculature has the potential to lead to malignant cell death and regression of macroscopic tumors, and the endothelial cell has, therefore, become an important target for anticancer drug development.[2]

Tubulin-interactive agents as a class have been shown to produce vascular damage and tumor cytotoxicity in animal studies, but these effects occurred at doses near the maximum-tolerated dose (MTD) and greater than those required for antimitotic activity.[3,4] Combretastatin A4 phosphate (CA4P) is a synthetic, water soluble, phosphorylated analog of combretastatin A4 (CA4), originally derived from the bark of the African willow *Combretum caffrum*.[5] CA4 binds tubulin at the colchicine-binding site and inhibits tubulin polymerization at micromolar concentrations.[6] CA4P is a prodrug that is rapidly converted to the active hydrophobic form CA4 by nonspecific phosphatases, some of which are overexpressed on endothelial cells in proliferating vasculature.[7,8] CA4P is selectively cytotoxic to proliferating human umbilical vein endothelial cells (HUVEC) in vitro but not to quiescent HUVECs or proliferating dermal fibroblasts.[9,10] In screens of cultured human cancer cells, CA4P shows reproducible antitumor activity but at concentrations substantially higher than those toxic to HUVECs.[11]

In vivo, this selective induction of endothelial cell apoptosis was found to create vascular shutdown and subsequent tumor necrosis and regression in murine and human tumor xenografts.[10,12] The antivascular effects occurred within 1 hour of CA4P administration, leading to a 100-fold reduction in blood flow at the center of tumors, with maintenance of control blood flow in most normal tissues studied in rats, including the heart, kidney, and small intestine.[12] Magnetic resonance imaging (MRI) proved to be a useful tool to study tumor perfusion in animal studies of CA4P.[13]

Animal toxicology studies of once-weekly and daily-times-five CA4P dosing revealed gastrointestinal hemorrhage or ulceration to be dose limiting; neutropenia, thrombocytopenia, bra-

From the University of Pennsylvania Cancer Center, Philadelphia, PA; Mary Babb Randolph Cancer Center, Morgantown, WV; Oxigene Inc, Boston, MA; and Gray Cancer Center, Norwood, United Kingdom.

Submitted December 12, 2002; accepted September 9, 2003.

Supported by a grant from Oxigene Inc, Boston, MA.

Presented at the American Association of Cancer Research Annual Meeting, San Francisco, CA, April 1-5, 2000.

Authors' disclosures of potential conflicts of interest are found at the end of this article.

Address reprint requests to James P. Stevenson, MD, University of Pennsylvania, 16 Penn Tower, 3400 Spruce St, Philadelphia, PA 19104; e-mail: james.stevenson@uphs.upenn.edu.

0732-183X/03/2123-4428/$20.00

DOI: 10.1200/JCO.2003.12.986

dycardia, and ventricular extrasystole were also noted.[14] Pharmacokinetic analyses using high-performance liquid chromatography revealed CA4P to be rapidly dephosphorylated to CA4 (half-life = 33 minutes), with CA4 glucuronide (CA4G) being the major biotransformation product. Clearance is predominantly via urinary excretion. Tumors were found to concentrate active CA4 to a greater degree than other tissues studied after CA4P administration.[12] This did not occur when CA4 alone was administered, indicating some degree of tumor selectivity after administration of the phosphorylated prodrug.

Therefore, we performed a phase I trial of CA4P administered as a 10-minute intravenous (IV) infusion for 5 consecutive days every 3 weeks to patients with advanced cancer. The starting dose for our study was 6 mg/m^2, which was less than one tenth the 10% severe toxicity dose in rats.

The pharmacodynamic end point of interest for CA4P and similar vascular targeting agents is the induced change in tumor blood flow and its relationship to toxicity and the pharmacokinetics of the drug and metabolites. Available methods for estimation of tumor blood flow include computed tomography, doppler ultrasound, positron emission tomography, and MRI. For this trial, we performed a preliminary investigation of tumor perfusion using serial dynamic contrast-enhanced MRI (DCE-MRI) in patients at the higher dose levels as a reproducible pharmacodynamic indicator of drug effect in tumor.

PATIENTS AND METHODS

Patients were treated on this trial between October 1998 and February 2000, at the Developmental Therapeutics Program of the University of Pennsylvania Cancer Center (Philadelphia, PA). All patients received therapy as outpatients. Eligible patients were at least 18 years of age with histologically confirmed solid tumors that were refractory to standard therapy or for which no effective therapy was available. An Eastern Cooperative Oncology Group performance status of ≤ 2 and a life expectancy of ≥ 12 weeks were required. All patients had recovered from prior treatment and had received no cytotoxic therapy or radiation in the previous 4 weeks (6 weeks for mitomycin or nitrosoureas). Patients had adequate bone marrow (absolute neutrophil count $\geq$ 1,500/μL, platelets $\geq$ 100,000/μL, and hemoglobin ≥ 9 g/dL), renal (creatinine ≤ 2 mg/dL or calculated creatinine clearance > 60 mL/min) and hepatic function (bilirubin within normal limits, transaminases $\leq 3 \times$ the upper limit of normal) at baseline. Patients were required to have no history of myocardial infarction in the previous 6 months, ECG findings that showed no clear evidence of ischemic heart disease, no evidence of gastrointestinal bleeding, and prothrombin times and calcium and magnesium within normal limits. Concomitant use of anticonvulsants, calcium channel blockers, antiarrhythmics, antianginal drugs, heparin, nonsteroidal anti-inflammatory drugs, and aspirin doses of greater than 100 mg daily was prohibited. The study was approved by the Institutional Review Board of the University of Pennsylvania, and all patients received information on the purpose and conduct of the study and signed written informed consent.

Pretreatment evaluation included a history and physical examination, CBC, serum electrolytes, creatinine, biochemical screen, and urinalysis within 2 weeks of initiating treatment, and documentation of the extent of disease (by computed tomography or MRI scanning) within 4 weeks. Chest radiograph and ECG were also performed before treatment. Blood counts were performed twice weekly, and biochemical profiles were performed weekly for the first cycle; patients were seen and examined before every course. Disease measurement was performed every other cycle. Toxicity during treatment was graded using National Cancer Institute common toxicity criteria, version 2.0. Response criteria were standard.[15]

As the study progressed, an episode of cardiotoxicity in a separate CA4P phase I trial at another institution prompted a more intensive monitoring schema with each course of treatment. All patients had placement of a continuous ECG monitor before treatment, and ECGs were obtained and reviewed hourly for 4 hours after beginning the infusion on day 1 and at 2-hour intervals in the succeeding days. Provisions were made for bedside monitoring in the event of any corrected QT interval greater than 500 ms, but this was not required.

Drug Administration

CA4P was supplied in 10-mL glass vials that contained 100 mg of lyophilized CA4P. The concentrated drug was reconstituted before use with 10 mL of sterile water, US Pharmacopeia, and further diluted with 0.9% sodium chloride to a final volume of 100 to 150 mL. The final volume was then administered daily as a zero-order IV infusion over 10 minutes on days 1 to 5. Cycles were repeated every 21 days.

Because of light sensitivity concerns, the administration sets were protected using foil, and the patient's immediate area and sample processing area were maintained free of fluorescent light. Only indirect incandescent yellow light was permitted.

Study Design

A modified Fibonacci escalation scheme was used in this trial. Three patients were accrued to each level until dose-limiting toxicity (DLT) was observed, whereupon expanded accrual to each level was used. The MTD was defined to be the dose at which one third or more of the patients experienced drug-related DLT. The recommended phase II dose was to be a well-tolerated dose below the MTD. DLT was defined as grade 4 neutropenia lasting ≥ 5 days or grade 3 to 4 neutropenia with sepsis, thrombocytopenia nadir less than 25,000/μL, or any nonhematologic toxicity grade ≥ 3 (excluding fatigue, alopecia, allergy, nausea, vomiting, or diarrhea in patients who had not received maximal symptom management). A treatment delay of more than 2 weeks and, as the study evolved, a heart rate corrected interval of either ≥ 500 ms or an increase $\geq 25\%$ over baseline were added as DLTs.

Pharmacokinetic Sampling and Analysis

The pharmacokinetics of CA4P and its primary metabolic products were evaluated on the first and fifth dose of cycle 1 at all dose levels studied. Thirteen serial blood samples were collected in each patient immediately before drug administration, 1 minute before the end of the infusion (10 minutes), and at the following times after infusion: 5, 15, 30, and 45 minutes, and 1, 1.5, 2, 4, 8, 12, and 24 hours. Simultaneously timed urine collections occurred in the following intervals: 0 to 4 hours, 4 to 8 hours, 8 to 12 hours, and 12 to 24 hours. Plasma samples were analyzed for parent CA4P, CA4, and CA4G. Urine samples were evaluated for CA4G. High-performance liquid chromatography methodology for the determination of CA4P, CA4, and CA4G concentrations was as described by Stratford and Dennis.[16]

All pharmacokinetic and pharmacodynamic analyses were performed using WINNonlin (Scientific Consultant, Apex, NC) Software (version 2.1; Pharsight, Corporation, Mountain View, CA). All patient CA4P, CA4, and CA4G plasma concentration-time data sets for each assessable dose were individually evaluated by a noncompartmental method, as described below. The absolute dose (nonnormalized) in micromoles was used as the input variable for all analyses. Because the molecular weight of CA4P is 440.3, doses given in mg were multiplied by 2.2712 to convert the values to micromoles.

Areas under the concentration-time curve (AUC) data provided in noncompartmental analyses were estimated by the linear trapezoidal rule with extrapolation using the 1/observed concentration^2 weight scheme for determination of the terminal elimination rate constant. One-way analysis of variance was performed to test whether the normalized AUC extrapolated to infinity and the maximal concentration (C_{max}) values for the active metabolite (CA4) increased with dose and whether there is any evidence of linearity. The test was generated using SAS version 8.0 (SAS Institute, Cary, NC) and a two-sided test at a significance level of .05.

DCE-MRI Imaging

MRI imaging was performed 3 to 5 days before initiation of CA4P treatment and 6 to 8 hours after completion of the day-5 dose. MRI imaging was performed on a 1.5 Tesla imaging system (Signa; GE Medical Systems, Milwaukee, WI). Imaging was performed with either a body coil or a phased array torso coil applied to the anatomy of interest. Initially, routine axial T1- and T2-weighted images were performed for localization of the patient's tumor. The largest observable lesion was then studied by DCE-MRI.

For native tumor T1 relaxation time measurement, an inversion-recovery prepared multiplanar fast gradient echo series was run with repeat time = 8.3 ms, echo time (TE) = 1.4 ms, and flip = 30 degrees. The following inversion times were run: 1,500 ms, 1,000 ms, 500 ms, and 500 ms with no inversion pulse. Breath-holding maneuvers were used at each inversion time for tumors in the chest or abdomen.

For DCE imaging, a suitable plane was chosen that allowed for maximal tumor coverage while avoiding the majority of pulsatility artifacts from the heart and aorta. For the majority of patients, we strove to avoid using an axial imaging plane so that out-of-plane tumor movement caused by variations in patient breath holding would be limited. Imaging used a three-dimensional fast spoiled gradient echo series with repeat time = 7.8 ms, TE = 4.2 ms, and flip angle = 30 degrees. We chose an in-phase TE of 4.2 ms to avoid paradoxical signal cancellation effects at fat-water interfaces.

Imaging field-of-view varied by patient but was generally 36 to 40 cm. Imaging matrix was 256 × 128. A slice thickness of 5 mm was used, with eight to 16 partitions, depending on the size of the tumor. This led to a nominal imaging time of 9 to 18 seconds for each run, excluding time between breath holds. Imaging was performed before and during rapid IV bolus administration of 20 mL of gadodiamide (Omniscan; Nycomed Imaging, Oslo, Norway) for a total of 5 to 7 minutes after contrast administration. Depending on patient respiratory reserve and number of imaging partitions, two or three images were acquired during each breath hold. In all cases, at least two images were obtained in direct succession during the anticipated first pass of contrast material to optimally characterize the up-slope of the dynamic enhancement curve.

DCE-MRI Analysis

Tumor regions of interest (ROIs) were manually drawn for each slice containing visible tumor by an experienced MRI radiologist (M.R.). In general, the images obtained during the first pass of contrast passage were used because these images demonstrated the greatest tumor-to-background tissue conspicuity. Visibly necrotic areas of tumor, as demonstrated on more delayed enhanced images, were excluded from the ROIs. The signal within these ROIs was averaged to obtain a mean tumor signal intensity at each inversion time (for tumor T1 relaxation time assessment) and at each postcontrast time point (for dynamic tumor enhancement assessment).

For T1 relaxation time measurement, the aggregate signal intensity for each tumor ROI was plotted versus inversion time. Data from the null inversion time was assigned a T1 value of both 0 and 10,000 ms. The data points for 0 and 500 ms were inverted below the baseline. Curve fitting to a single exponential equation with three parameters (T1 value, maximum signal intensity, and offset) was then performed to estimate tumor T1 relaxation time.

Whole-tumor dynamic gadolinium concentration curves were generated using the signal enhancement ratio and the baseline tumor T1 relaxation time, assuming linear dependence between gadolinium concentration and change in water relaxivity.[17] These resulting time courses of gadolinium transfer into the tumor interstitium were then subjected to nonlinear least squares fitting based on the two-compartment kinetic model of Tofts and Kermode.[18] This analysis yields two kinetic parameters, K^{tr} and V^e. K^{tr} is the rate of transfer of gadolinium (and other small molecular weight tracers) between the plasma and the tumor interstitial compartment. The physiologic interpretation of K^{tr} can vary.[19] In cases where blood flow is rapid, K^{tr} represents the microvessel permeability-surface area product. However, in cases of extremely high permeability or when tumor blood flow is low, K^{tr} reverts to the tumor blood flow. In cases with both reasonably high blood flow rates and vessel permeability, as can be expected in most tumors, K^{tr} reflects a combination of both blood flow and the permeability-surface area product. The second derived parameter, V^e, reflects the volume fraction of tumor extravascular, extracellular space. Curve fitting was performed on in-house–derived routines using the IDL software package (Research Systems Inc, Boulder, CO).

Correlation Between Pharmacokinetic and Pharmacodynamic Data

The relationships between pharmacodynamic and pharmacokinetic parameters were assessed. Absolute and relative changes in the two pharmacodynamic parameters (K^{tr} and V^e) were plotted versus CA4P dose and against C_{max} and AUC for both CA4P and CA4. Correlation was assessed with the Pearson's product moment correlation coefficients. Significance of correlation was assessed at the $P = .05$ level.

RESULTS

Patient Characteristics

A total of 37 patients received 133 cycles of CA4P as part of this trial. All patients were assessable for toxicity. Two patients received only day 1 of treatment and were removed from the study as a result of toxicity, as described below, and a patient with metastatic osteogenic sarcoma discontinued CA4P treatment after day 3 because of rapidly progressing disease. The demographic characteristics of the patients are listed in Table 1. There was a preponderance of males, with a median age of 55 years. All but one patient had received prior chemotherapy. The performance status of these patients was excellent, with all patients having an Eastern Cooperative Oncology Group performance status of 0 or 1. A range of solid tumors was represented among patients receiving therapy, with nearly 25% of patients having sarcomas of the soft tissues or bone.

Dose Levels

The doses studied and the number of patients per dose level are listed in Table 2. Each dose level represents the CA4P dose

Table 1. Patient Characteristics

Characteristic		No. of Patients (N = 37)
No. of assessable patients		37
Age, years		
Mean	52	
Range	19-89	
Sex		
Male		26
Female		11
Performance status		
0		12
1		25
Prior treatment		
Chemotherapy		23
Radiation		15
None		1
Tumor type		
Sarcoma		9
Colorectal		7
Lung, non–small-cell		6
Renal		4
Thyroid		4
Pancreatic		2
Other		5

Table 2. Dose Escalation Strategy

Dose (mg/m^2)	No. of Patients	No. of Cycles
6	3	12
12	3	5
20	3	7
30	3	6
42	3	10
56	3	14
75*	6	10
65	6	48
52	7	21

*Maximum-tolerated dose.

administered daily for 5 consecutive days repeated every 3 weeks. Expansion of dose levels as a result of DLT did not occur until the 75-mg/m^2 level was reached, and when this was found to be the MTD, accrual to the intermediate dose of 65 mg/m^2 followed. Subsequent investigation of a lower dose level (52 mg/m^2) was pursued to further characterize what was being considered as the recommended phase II dose level. Consistent with our previous results, we found this dose also to be well tolerated.

Hematologic Toxicity

No significant hematologic toxicity was observed with CA4P treatment. One heavily pretreated patient with soft tissue sarcoma developed grade 2 thrombocytopenia in cycle 1. Besides this lone exception, there were no episodes of grade 2 or greater neutropenia or thrombocytopenia in cycle 1, and for patients who went on to receive more than two cycles, there was no evidence of cumulative hematologic effects.

Nonhematologic Toxicity

CA4P was remarkably well tolerated at doses less than 50 mg/m^2. Nonhematologic toxicities became apparent only at doses above this threshold (Table 3). The most severe side effect was infusion-associated pain at sites of known tumor or metastases. We found this to be dose-limiting at the 75-mg/m^2 level because two of six patients developed grade 3 pain at this dose. By common toxicity criteria, grade 3 tumor pain is considered severe, such that the pain or analgesics severely interferes with activities of daily living, whereas grade 4 pain is disabling. Although the sites of these painful episodes varied depending on tumor(s) location, the timing and characteristics of the pain was fairly uniform. The pain usually occurred within 1 hour of completion of each CA4P infusion, reaching crescendo 1 to 2 hours after onset and finally abating within 6 to 8 hours. The location of the pain tended to be in sites of known bulky visceral disease, including lung and liver. The pain was usually severe enough to require treatment with oral or parenteral narcotics. Most patients responded to treatment, but narcotic pretreatment with subsequent doses or cycles did not prevent its occurrence or severity. This toxicity seemed to be dose-related, with two of seven patients at the 52-mg/m^2 dose level experiencing grade 2 pain, one patient at the 65-mg/m^2 level experiencing grade 3 pain, and two patients at the 75-mg/m^2 level experiencing pain as noted earlier. The two episodes of grade 3 tumor pain at 75 mg/m^2 and the cardiopulmonary toxicity described below established 75 mg/m^2 as the MTD according to the protocol design. Only four of six patients at the 75-mg/m^2 dose were able to complete the initial 5 days of CA4P dosing.

A range of other seemingly neurologic effects was observed, and these effects varied in incidence and severity, with a wide range of manifestations. Grade 1 and 2 neurosensory effects were not uncommon and, in most patients, took the form of perineal/perirectal paresthesias that were transient and occurred near the end of infusion. More classic stocking-glove sensory effects were observed as well. These symptoms were short-lived and not cumulative in nature. Headache was also observed at higher doses (also grade 1 and 2) but was more delayed in onset because it tended to occur in the evening more than 6 hours after dosing and generally resolved by the following morning. Grade 1 and 2 neuromotor toxicity was observed in four patients at higher dose levels. In two patients, this took the form of lower extremity weakness, whereas the other two patients experienced cerebellar ataxia, which was also more pronounced in the lower extremities. This toxicity was most severe (grade 2) in one patient with rectal cancer treated with 75 mg/m^2; the timing was similar to that of headache, but symptoms persisted into the morning of day 2 of treatment, and the patient was removed from study because it was feared that further dosing would worsen this

Table 3. Cycle 1 Grade 2 or Greater Nonhematologic Toxicity by Dose Level

Dose (mg/m^2/d)	No. of Patients																		
		Nausea or Vomiting Grade			Tumor Pain Grade			Syncope Grade			Neurosensory Grade			Dyspnea Grade			Headache Grade		
	Total	2	3	4	2	3	4	2	3	4	2	3	4	2	3	4	2	3	4
6.0	3	—	—	—	—	—	—	—	—	—	—	—	—	—	—	—	—	—	—
12	3	1	—	—	—	—	—	—	—	—	—	—	—	—	—	—	—	—	—
20	3	—	—	—	—	—	—	—	—	—	—	—	—	—	—	—	—	—	—
30	3	—	—	—	—	—	—	—	—	—	—	—	—	—	—	—	—	—	—
42	3	—	—	—	—	—	—	—	—	—	—	—	—	—	—	—	—	—	—
52	7	—	—	—	2	—	—	—	—	—	—	—	—	—	—	—	—	—	—
56	3	—	—	—	—	—	—	—	—	—	—	—	—	—	—	—	—	—	—
65	6	1	—	—	—	1	—	—	—	—	—	—	—	—	1*	—	1	—	—
75	6	3	1	—	—	2*	—	—	1*	—	2	—	—	—	—	1*	1	—	—

*Dose-limiting toxicity.

Table 4. CA4P Pharmacokinetic Parameters: Day 1 AUC_{inf} Values for CA4P, CA4, and CA4G

CA4P Dose (mg/m^2)	No. of Patients	CA4P AUC_{inf} ($\mu m \cdot h$)		CA4 AUC_{inf} ($\mu m \cdot h$)		CA4G AUC_{inf} ($\mu m \cdot h$)	
		Mean	SD	Mean	SD	Mean	SD
6	3	1.64	0.2	0.31	0.1	4.82	1.1
12	3	2.27	0.9	0.42	0.1	6.15	2.3
20	3	3.61	0.8	0.76	0.3	9.25	1.4
30	3	3.04	1.3	1.54	1.3	17.59	8.9
42	3	4.58	0.8	0.82	0.4	16.79	9.7
52	7	9.38	1.8	2.1	0.6	23.84	10.4
56	3	11.98	5.4	2.22	0.4	29.04	6.3
65	6	10.76	4.1	2.24	0.6	30.46	11.3
75	6	16.35	5.2	3.48	0.9	41.21	18.9

Abbreviations: AUC_{inf}, area under the concentration-time curve extrapolated to infinity; CA4P, combretastatin A4 phosphate; CA4, combretastatin A4; CA4G, combretastatin A4 glucuronide; SD, standard deviation.

troubling side effect. An MRI of the brain revealed no abnormalities. This individual's motor function returned to baseline within 1 week of treatment. Of note, all of the patients experiencing neuromotor toxicity had received prior platinum agents (cisplatin, n = 3, and oxaliplatin, n = 1).

Cardiopulmonary DLT occurred in two patients treated at 75 mg/m^2. One patient with non–small-cell lung cancer and pulmonary metastases experienced grade 4 dyspnea after his first dose of CA4P in cycle 1 and was withdrawn from the study. Attribution of this toxicity was complicated by the fact that this patient with lung cancer was found to have unsuspected poor baseline pulmonary status and had been using supplemental oxygen on a regular basis at home, and his symptoms resolved promptly with the addition of oxygen by nasal cannula. The patient described earlier who developed ataxia also had a dose-limiting syncopal episode in the setting of grade 2 hypotension and grade 3 hypoxia (as measured by pulse oximetry) after his first and only dose of CA4P. The syncope was judged to be a consequence of the hypotension, which also complicated the interpretation of the pulse oximetry values. The hypotension and his symptoms responded quickly to IV hydration.

Concerns regarding corrected QT interval prolongation prompted close attention to rhythm or ECG abnormalities during treatment. Despite intensive monitoring with serial ECGs (all independently reviewed) and continuous ECG monitoring (in patients treated at 52 mg/m^2), we observed no other cardiac toxicities and found no abnormalities such as arrhythmias or ischemic changes.

Other nonhematologic toxicities were mild and included nausea and vomiting, which responded to therapy and prophylaxis with 5-hydroxytryptamine-3–receptor antagonists, and grade 1 and 2 fatigue. Transient serum lactate dehydrogenase elevations were noted in week 1 in multiple patients. No treatment-related alopecia was observed.

Pharmacokinetic Analyses

A total of 37 patients were entered onto this study and had pharmacokinetic samples collected on the first dose of the first course. Thirty-two of the 37 patients also had samples collected for pharmacokinetic studies on the fifth dose of course 1. Mean AUC values for CA4P, CA4, and CA4G by dose level are listed in Table 4.

Plasma CA4P pharmacokinetics. The mean terminal half-life of CA4P was 0.36 hours on the first dose and 0.22 hours on the fifth dose, as estimated from at least three time points. The mean volume of distribution at steady-state value was 5.6 L on dose 1 and 4.5 L on dose 5. The mean systemic clearances of CA4P were 28.2 L/h and 29.5 L/h on doses 1 and 5, respectively. The mean intrapatient difference between the two clearance values was 16% (median, 12%; range, 0.3% to 77%). A typical CA4P, CA4, and CA4G concentration versus time plot for one patient treated with 52 mg/m^2 is shown in Fig 1.

CA4P AUC and C_{max} values increased in a dose-linear fashion over the 13-fold range studied. No evidence of nonlinearity was found in CA4P terminal half-life or systemic clearance across dose levels. No evidence was discovered for accumulation of CA4P on dose 5 compared with dose 1 because pretherapy values were consistently below the limits of detection, as anticipated from the elimination half-life. Systemic clearance values of CA4P on dose 1 and 5 were highly correlated (r^2 = 0.79) and similar.

Dose-normalized CA4P AUC and C_{max} values did not appear different per dose level and one-way analysis of variance results showed that none of the tests were significant at level $\alpha = 0.05$.

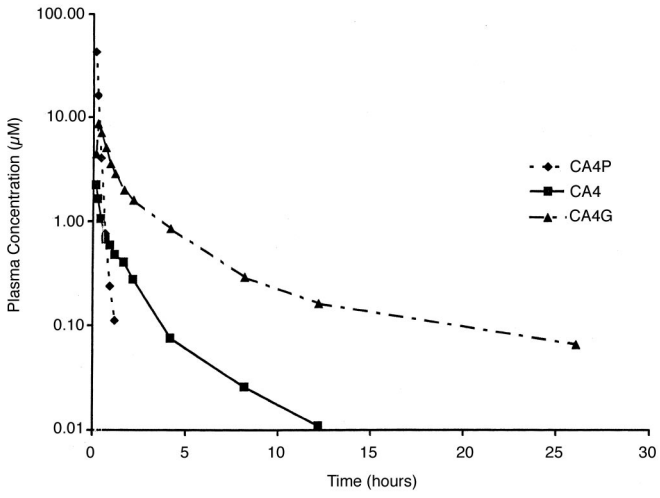

Fig 1. Plasma concentration versus time curves for combretastatin A4 phosphate (CA4P), combretastatin A4 (CA4), and CA4 glucuronide (CA4G) in a patient treated at the 52-mg/m^2 dose level.

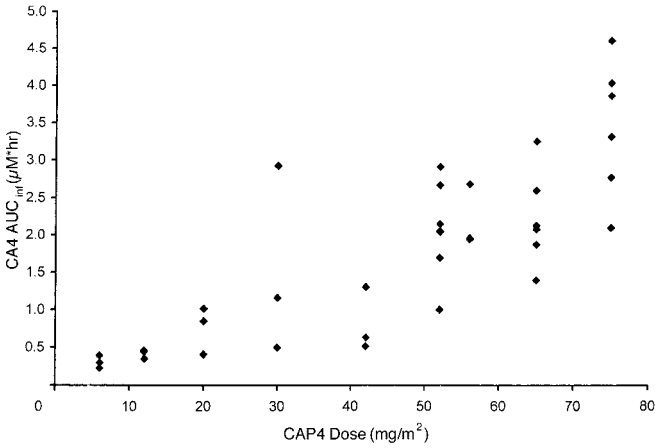

Fig 2. Combretastatin A4 (CA4) area under the concentration-time curve (AUC) versus CA4 phosphate (CA4P) dose level.

No substantial association was found between unnormalized parent drug clearance and patient body-surface area ($r^2 = 0.08$).

Plasma CA4 pharmacokinetics. The CA4 mean terminal half-life was 3.3 hours on both dose 1 and 5, as estimated from at least three time points. As anticipated, the half-life of CA4 is much longer than the half-life observed with the parent drug. The half-life of the parent drug and CA4 did not seem to be associated.

CA4 AUC and C_{max} values increased in a dose-linear fashion over the 13-fold range studied (Fig 2). CA4 accumulation was not evident when comparing its AUC on dose 1 versus dose 5. No evidence of nonlinearity was found in CA4 terminal half-life across dose levels. A directly proportional relationship was observed between CA4P AUC and CA4 AUC values. A slight association was found between the CA4P C_{max} and the CA4 C_{max}.

CA4G was readily detected in urine samples obtained after administration of the dose. A mean of 63% of the CA4P dose was excreted as CA4G in the first 24 hours of urine collection after the first dose, and a mean of 60% was extracted after the fifth dose. Actual values varied over a two- to four-fold range, with a coefficients of variation of 16% to 22%.

Tumor Perfusion by DCE-MRI

A total of 15 patients were studied by DCE-MRI before and after week 1 of CA4P administration, 10 of whom yielded analyzable DCE-MRI data. Tumor sizes ranged from approximately 1 cm to over 10 cm. Reasons for failure to achieve interpretable data included small size of tumor (n = 1), severe cardiac or respiratory ghost artifacts (n = 3), and MRI equipment failure (n = 1).

Tumor sizes and T1 measurements are listed in Table 5. In one patient, a reliable T1 measurement could not be made on the postCA4P examination because of excessive patient motion. A uniform T1 measurement was assumed for both pre- and postCA4P imaging sessions for this patient. Although tumor T1 measurements showed a wide variation (ranging between 622 ms and 1,142 ms), no individual tumor T1 relaxation time changed by more than 20% between visits. The majority of the tumors either exhibited stable or slightly increased T1 on the post-therapy study. Two tumors demonstrated a small decrease in T1 relaxation time at the time of follow-up study.

Given the heterogeneity in tumor types studied, there was a marked variation in the baseline (preCA4P) DCE-MRI tumor perfusion parameters. Baseline and postCA4P results for all 10 patients with interpretable DCE-MRI data are listed in Table 6. Inspection of these values reveals that there were several examples of highly vascular tumors (eg, thyroid) that demonstrated rapid contrast uptake, yielding large DCE-MRI perfusional parameters. Other tumors were more hypovascular, yielding lower DCE-MRI values. Although none of the tumors demonstrated large areas of frank necrosis, several of the more hypovascular tumors demonstrated extensive central areas that were poorly perfused and weakly enhancing.

In eight of 10 patients, there was at least a mild decrease in the K^{tr} value; three patients demonstrated marked loss of vascularity after CA4P. Tumors with the largest baseline enhancement demonstrated the greatest drop in K^{tr} after CA4P ($r = -0.89$, $P < .001$); this was noted in three patients with papillary thyroid, medullary thyroid, and rectal carcinoma. This effect is illustrated in Fig 3. There was a more consistent pattern of alteration in tumor leakage space (V^e) after CA4P, with seven of 10 patients demonstrating a decrease in accessible volume fraction of at

Table 5. Tumor Characteristics and T1 Values of Patients Studied With DCE-MRI

Patient No.	Age (years)	CA4P Dose (mg/m^2)	Tumor Type	Lesion Examined	Size (cm × cm)	Tumor T1 Before CA4P (ms)	Tumor T1 After CA4P (ms)
1	48	52	Melanoma	Lung metastasis	4.0 × 3.9	859	—*
2	39	52	Penile; leiomyosarcoma	Nodal metastasis (perineum)	3.4 × 2.1	1,004	973
3	31	52	Osteosarcoma (hip)	Locally recurrent tumor	8.5 × 6.5	872	896
4	71	65	NSC lung	Lung mass	3.3 × 3.8	814	970
5	45	65	Thyroid	Osseous metastasis (sacrum)	6.3 × 6.1	746	874
6	19	65	Thyroid	Nodal metastasis (neck)	2.5 × 3.1	821	794
7	60	65	Colon	Liver metastasis	13.5 × 11.1	766	900
8	49	75	Small bowel	Liver metastasis	3.1 × 3.8	722	769
9	54	75	Rectal	Lung metastasis	2.8 × 3.8	930	1,000
10	54	75	Pancreas	Liver metastasis	4.6 × 3.6	829	700

Abbreviations: DCE-MRI, dynamic contrast-enhanced magnetic resonance imaging; CA4P, combretastatin A4 phosphate; NSC, non–small-cell.
*T1 value not obtainable because of excessive image noise or patient motion. The preCA4P value was used for both DCE-MRI examinations.

Table 6. Baseline and PostCA4P Tumor Perfusion Parameters for All 10 Patients With Interpretable DCE-MRI Data

Tumor Type	CA4P Dose (mg/m^2)	K^{tr} (min^{-1})		V^e	
		PreCA4P	PostCA4P	PreCA4P	PostCA4P
Melanoma	52	1.31	0.93	0.38	0.34
Leiomyosarcoma	52	0.25	0.19	0.33	0.33
Osteosarcoma	52	0.63	0.20	0.28	0.16
Lung (NSC)	65	0.42	0.29	0.35	0.16
Thyroid	65	3.32	1.05	0.79	0.66
Thyroid	65	3.17	0.82	0.72	0.35
Colon	65	0.75	0.96	0.22	0.23
Small bowel	75	0.44	0.19	0.51	0.32
Rectal	75	3.27	2.16	0.34	0.16
Pancreas	75	0.69	1.10	0.69	0.52

Abbreviations: CA4P, combretastatin A4 phosphate; DCE-MRI, dynamic contrast-enhanced magnetic resonance imaging; K^{tr}, transferrate of gadolinium between the plasma and interstitial compartment; V^e, volume fraction of tumor extravascular, extracellular space; NSC, non–small-cell.

least 10% and no patient demonstrating a significant increase in leakage space.

In one patient, there was a dramatic visual change in the pattern of tumor enhancement. This patient, who had metastatic thyroid cancer, demonstrated striking segmental devascularization of a portion of a large sacral metastasis after day 5 of CA4P dosing. This is illustrated in Fig 4, where the early arterial phase images from a single slice are shown before and after therapy. As can be seen, there is subsequent absence of enhancement in a large inferior portion of the tumor.

Correlation Between DCE-MRI Response and CA4P Pharmacokinetics

No correlation was noted between alteration in the plasma-tumor gadolinium exchange rate and CA4P dose (Fig 5A); however, there was a moderate negative correlation with the day 5 CA4P C_{max} and AUC values (Fig 5B and 5C) and a significant negative correlation ($r = 0.549$, $P = .05$) between change in K^{tr} and the day 5 CA4 AUC (Fig 5D). Of note in Fig 5D, there seemed to be one outlier value with the highest CA4 AUC and greatest negative change in K^{tr}. A negative correlation between change in K^{tr} and CA4 C_{max} was not observed.

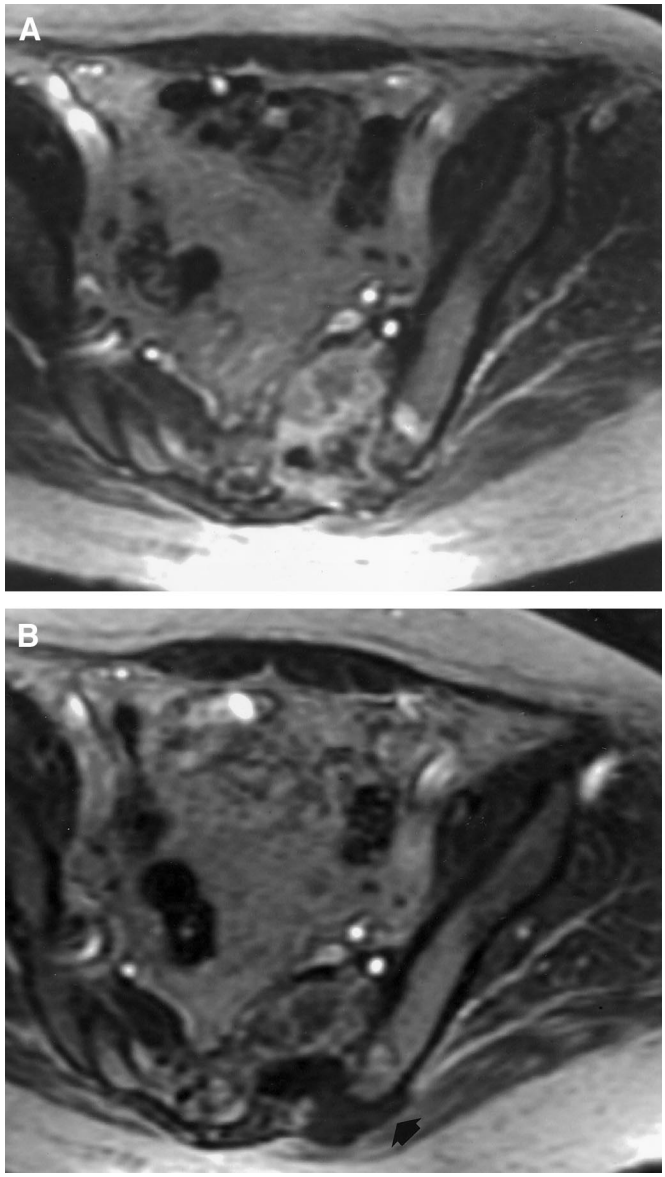

Fig 4. Dynamic contrast-enhanced magnetic resonance images showing a decline in perfusion of a sacral metastasis in a patient with papillary thyroid cancer. Delayed postgadolinium T1-weighted images (A) before and (B) 1 week after CA4P treatment. In B, note the absence of enhancement in the inferior portion of the tumor (arrow).

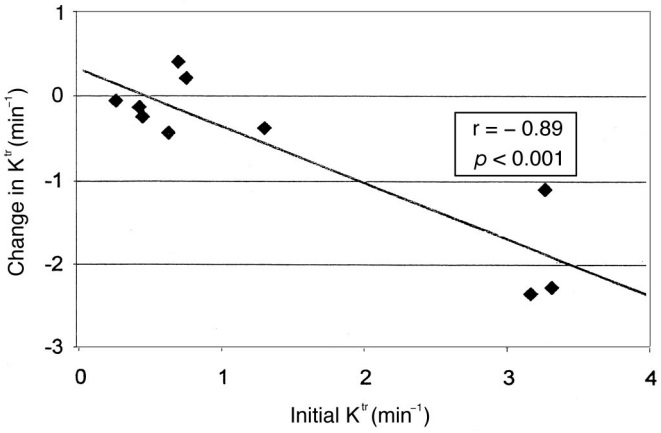

Fig 3. Correlation between initial tumor perfusion (K^{tr}) and change in K^{tr} in patients studied with serial magnetic resonance imaging.

Interestingly, although there was a trend between reduction in tumor V^e and CA4P dose ($r = -0.48$, $P = .08$), there was no consistent trend between reduction in tumor V^e and pharmacokinetic indices of CA4P and CA4. This finding may reflect the presence of macroscopic (segmental) tumor vascular shutdown that is independent of CA4P dose and is instead influenced by the relative stability or immaturity of tumor vascular networks.

Patient Benefit

Fifteen patients received more than two cycles of CA4P as a result of disease stabilization or improvement. One patient with

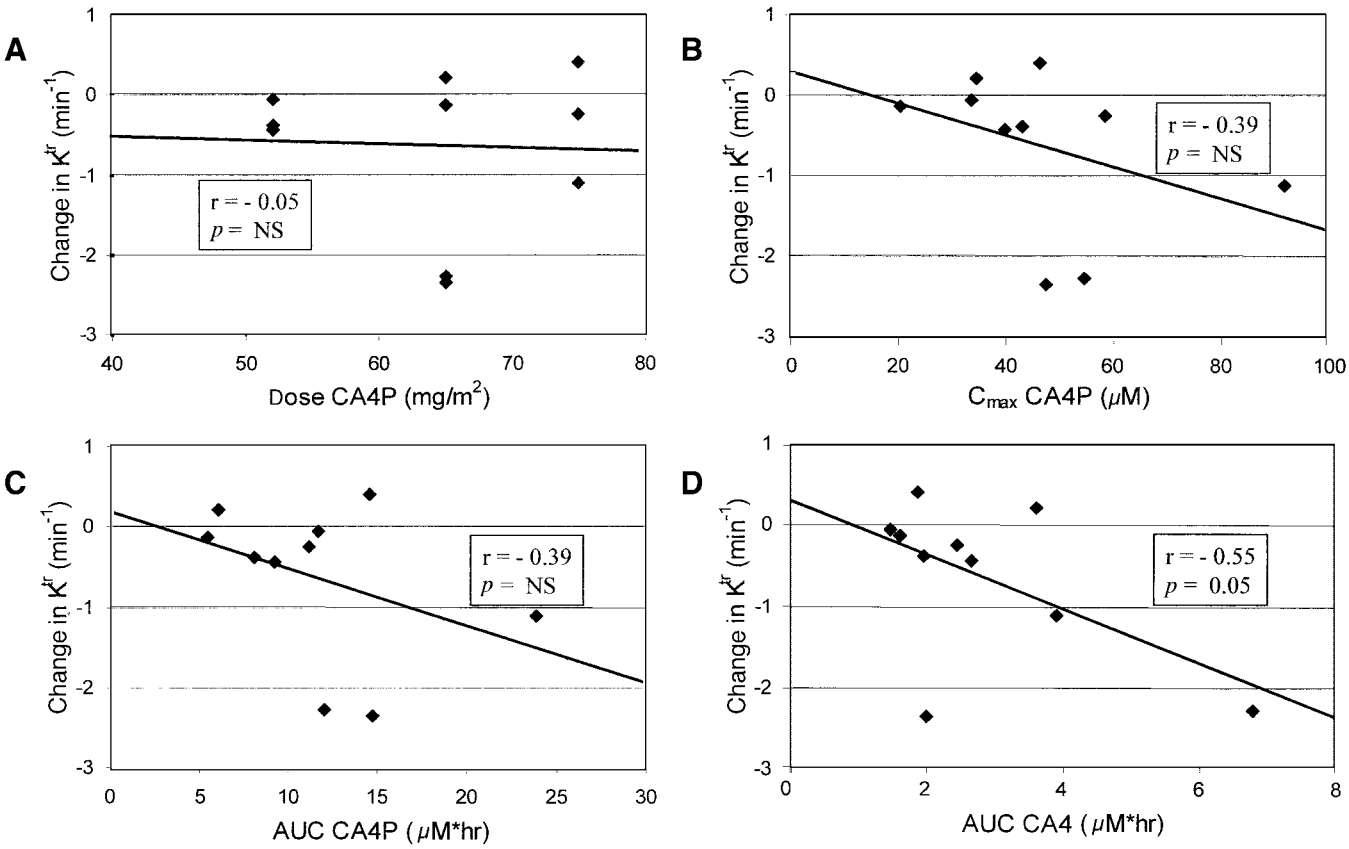

Fig 5. Relation between alterations in tumor first-order rate constant of gadolinium (K^{tr}) and combretastatin A4 phosphate (CA4P) pharmacokinetic indices. Change in K^{tr} versus (A) dose CA4P, (B) C_{max} CA4P, (C) area under the concentration-time curve (AUC) CA4P, and (D) AUC CA4. Negative K^{tr} values reflect loss of perfusion after CA4P treatment. NS, not significant.

heavily pretreated metastatic fibrosarcoma who received 56 mg/m^2 had a partial response in multiple pulmonary metastases and received eight cycles before progression. Another 14 patients maintained disease stability lasting three to 29 cycles. Most notable was a remarkable 19-year-old male with metastatic medullary thyroid carcinoma who received 29 cycles of CA4P. He had received prior therapy with the investigational agent TNP-470, and his sites of progressive metastatic disease included the lungs and hila/mediastinum. Minor response was noted in the areas of adenopathy. He developed no significant cumulative toxicity during his treatment course and discontinued therapy only after eventual progressive disease was observed.

DISCUSSION

We found CA4P to be reasonably well tolerated at doses of 52 to 65 mg/m^2 when administered as a bolus infusion for 5 consecutive days, and we also noted antitumor activity in this dose range. The finding of tumor pain as the DLT in this trial was unequivocal, and its appearance and severity were dose dependent. The fact that we were unable to expand the 65-mg/m^2 dose level to more than six patients because of noted concerns raises the possibility that this dose may exceed the MTD because DLT was observed at this level and drug clearance was variable. Cardiac toxicity observed with CA4P doses above 56 mg/m^2 in a separate phase I study[20] would, therefore, lead us to recommend the 52-mg/m^2 dose for further phase II evaluation on this schedule.

Pain at tumor sites has been well described after treatment with antimicrotubule drugs, both those currently used in standard practice as well as experimental agents in recent phase I trials.[21-24] Tumor pain has also been apparent in other single-dose phase I trials of CA4P.[20,25] Although the phenomenon is readily apparent, its underlying mechanism is less apparent. The neurotoxicity that is broadly associated with these drugs as a class would lead to speculation that this may be a manifestation of an acute neuropathic effect; however, the antivascular basis for the development of these agents raises the distinct possibility that pain may be a consequence of reduced tumor blood flow.[26] The vascular shutdown documented with CA4P treatment in vivo should, therefore, suggest a similar cause and effect relationship. A detailed investigation of such a relationship was beyond the scope of this trial, and further clinical experience with CA4P and related compounds will be needed to better characterize the pharmacodynamics of tumor pain (ie, certain visceral sites of tumor and metastasis may be more likely to produce pain after treatment). Unfortunately, tumor pain did not seem to correlate with radiographic evidence of tumor response in individual patients, and we found no pharmacodynamic

association between CA4P and CA4 pharmacokinetic parameters and this toxicity. Furthermore, the time-course of the altered perfusion was not studied in this trial, but investigators in the United Kingdom showed persistence of the blood supply impairment for at least 24 hours.[25] Therefore, a simple relationship between the pain and perfusion changes is unlikely.

Interestingly, CA4P did not produce significant hematologic toxicity, which sets it apart from the commonly used vinca alkaloids and taxanes, as well as colchicine.[27] Other effects were more heterogeneous and predominated at the higher dose levels. CNS toxicity, such as headache and ataxia, lower extremity weakness, and transient sensory neuropathy (notably in the pelvis and perineum), nausea, and dyspnea were observed. These findings suggest that CA4P effects are not limited solely to the targeted proliferating endothelium of tumors and that perhaps they were a consequence of reduced perfusion of certain normal tissues. Microtubule depolymerization is known to affect arteriolar vasomotor tone, a finding reported to be independent of endothelial effects; other preclinical reports have shown that CA4P is not tumor specific and is toxic to proliferating endothelium in normal organs, such as the thyroid gland, and can reduce blood flow to the brain.[12,28,29] These studies indicate that there may be multiple mechanistic explanations for the range of side effects we observed with CA4P treatment.

Again, the variety of toxicities observed across individual patients makes identification of specific determinants of these effects difficult. Of interest was the fact that that the four patients who experienced neuromotor toxicity had received prior platinum therapy. Cisplatin is known to damage normal endothelium and, in theory, may predispose patients receiving an endothelial toxin, such as CA4P, to greater side effects.[30,31] Further experience with CA4P in the clinic will be crucial to the demonstration of its safety when used in platinum-pretreated patients or in combination with platinum drugs.

Our experience with DCE-MRI as part of this trial was valuable and yielded results of interest. The growing role for the use of serial MRI examinations to measure tumor perfusion as part of clinical trials with antivascular agents provides an important noninvasive pharmacodynamic marker of effect.[32] The further refinement of imaging techniques and methods of analysis is likely to prove critical in pharmacodynamic assessments of efficacy as well as to provide proof of mechanism in future trials of the multitude of antiangiogenic and antivascular agents under study. Novel DCE-MRI techniques are under investigation in attempts to characterize tumor neovasculature in regard to fractional blood volume and mean vessel size.[33] The advent of macromolecular magnetic resonance contrast agents may lead to further developments in the use of imaging to evaluate and differentiate the effects of various antivascular agents on bulk tumor blood flow and microvessel permeability.[34]

Other investigations, such as serial tumor biopsies and assessments of wound healing, have been reported in antiangiogenesis trials with varying results.[35,36] Imaging modalities, such as DCE-MRI, represent a less-invasive means to study vascular end points and may be more broadly applicable. Our results were not uniform and shed light on some of the pitfalls of integrating this technology into clinical trials. The intrinsic variability of tumor vasculature yields challenges regarding the quantification of tumor vascular inhibition in clinical trials of antivascular agents. In patients with relatively hypovascular tumors, small alterations in perfusion may be difficult to detect. Larger tumors often present with dominant areas of central hypovascularity. DCE-MRI parameters of such tumors may be dominated by the kinetic indices of the hypovascular regions, obscuring clinically significant antivascular effects occurring at the tumor margins. Analyses that look at regional or point-by-point variation in tumor perfusion may overcome these difficulties.[37] Unfortunately, many patients with imageable disease demonstrate tumors in anatomic areas that are susceptible to respiratory and cardiac motion, complicating any such analysis. Physiologic (eg, cardiovascular) variation can alter kinetic parameters obtained with DCE-MRI measurements. However, reproducibility studies have suggested that the intrapatient variability of such measurements for tumors is much less than the interpatient variability.[38] This is especially true for V^e measurements, which seem to be reproducible to within 10%, even without explicit measurement of arterial input functions.

We obtained extremely large values for both K^{tr} and V^e in several highly vascular tumors. In particular, V^e values in excess of 70% were obtained, suggesting that these tumors are composed of less than 30% intracellular space by volume. Tumors are known to demonstrate larger extracellular spaces, relative to that of normal tissue, because of disorganized cellular growth patterns. However, the more extreme values obtained in our study were higher than expected. This suggests that the two-compartmental model we used may not be fully representative of the tumor gadolinium kinetics. Our kinetic enhancement data was not of sufficiently high temporal resolution to allow us to attempt fitting with more complex multicompartmental models (including those with nonnegligible intravascular volume fractions). The original compartment model of Tofts and Kermode[18] was derived for the study of inflammatory lesions of the CNS. Enhancement kinetics of these CNS lesions were likely of the degree that would allow for accurate two-compartment modeling without regard to the likely negligible intralesional vascular volume.

Tumor location is an additional confounding variable when addressing the inhibitory effects of tumor vasculature by agents such as CA4P. Tumor milieu (eg, lung *v* liver *v* bone marrow) may play an important role in defining the type and resiliency of tumor neovasculature. Patients often present with a combination of primary tumor and distant metastases, often in multiple locations. Our imaging protocol allowed for dynamic blood flow analysis of only the most dominant lesion. As such, variability of tumor response within a given patient could not be assessed in this study. Nevertheless, despite these obstacles in performing and quantitating DCE-MRI effects, we found promising evidence of diminished tumor perfusion after CA4P therapy in individual patients, with positive correlation between degree of tumor vascular inhibition and CA4P pharmacokinetics. We are currently continuing study of DCE-MRI in trials of CA4P and other agents at our institution.

Pharmacokinetic analyses performed in this trial revealed the plasma disposition of CA4P after infusion to be similar to that observed in animal studies. CA4P and CA4 AUC and C_{max} values were found to increase with dose, and clearance was linear across dose levels. The finding that no plasma accumulation occurred from day 1 to day 5 was consistent with the toxicities observed during the dosing week because these toxicities tended to be of similar severity with each CA4P dose. However, the lack of association between body-surface area and CA4P clearance would suggest that body-surface area–based dosing may not be the most appropriate way to administer CA4P in the clinic. Further exploration of alternative dosing methods seems warranted.

Finally, the evidence of antitumor efficacy we observed with CA4P treatment proved encouraging. In addition to the single partial response, the number of patients with prolonged disease stability was encouraging in a phase I trial of patients with pretreated and resistant tumor types. The fact that one patient with medullary thyroid carcinoma received a remarkable 29 cycles of CA4P without cumulative toxicity was also reassuring. Our results coupled with a finding that CA4P enhanced the effect of doxorubicin against medullary thyroid carcinoma in vivo would indicate that this tumor in particular is worthy of further study in trials of CA4P alone and in combination.[39] Reports have also demonstrated synergism between CA4P and radiotherapy, as well as other chemotherapeutic agents such as fluorouracil.[40,41] These findings of clinical efficacy support the further development of this class of agent.

AUTHORS' DISCLOSURES OF POTENTIAL CONFLICTS OF INTEREST

The following authors or their immediate family members have indicated a financial interest. No conflict exists for drugs or devices used in a study if they are not being evaluated as part of the investigation. Owns stock (not including shares held through a public mutual fund): David Chaplin, Oxigene (Boston, MA), and Scott L. Young, Oxigene. Served as an officer of the Board of a company: David Chaplin, Oxigene, and Scott L. Young, Oxigene.

REFERENCES

1. Folkman J: Angiogenesis in cancer, vascular, rheumatoid and other disease. Nature Med 1:27-31, 1995
2. Denekamp J: Angiogenesis, neovascular proliferation, and vascular pathophysiology as targets for cancer therapy. Br J Radiol 66:181-196, 1993
3. Hill SA, Lonergan SJ, Denekamp J, et al: Vinca alkaloids: Anti-vascular effects in a murine tumor. Eur J Cancer 29A:1320-1324, 1993
4. Hill SA, Sampson LE, Chaplin DJ: Antivascular approaches to solid tumor therapy: Evaluation of vinblastine and flavone acetic acid. Int J Cancer 63:119-123, 1995
5. Pettit GR, Singh SB, Hamel E, et al: Isolation and structure of the strong cell growth and tubulin inhibitor combretastatin A-4. Experientia 45:209-211, 1989
6. Woods JA, Hadfield JA, Pettit GR, et al: The interaction with tubulin of a series of stilbenes based on combretastatin A-4. Br J Cancer 71:705-711, 1995
7. Pettit GR, Temple C, Narayanan VL, et al: Antineoplastic agents 322. Synthesis of combretastatin A-4 prodrugs. Anticancer Drug Des 10:299-309, 1995
8. Tozer GM, Kanthou C, Parkins CS, et al: The biology of the combretastatins as tumour vascular targeting agents. Int J Exp Pathol 83:21-38, 2002
9. Dark GD, Hill SA, Prise VE, et al: Combretastatin A-4, an agent that displays potent and selective toxicity toward tumor vasculature. Cancer Res 57:1829-1834, 1997
10. Iyer S, Chaplin DJ, Rosenthal DS, et al: Induction of apoptosis in proliferating human endothelial cells by the tumor-specific antiangiogenesis agent combretastatin A-4. Cancer Res 58:4510-4514, 1998
11. Grosios K, Holwell SE, McGown AT, et al: In vivo and in vitro evaluation of combretastatin A-4 and its sodium phosphate prodrug. Br J Cancer 81:1318-1327, 1999
12. Tozer GM, Prise VE, Wilson J, et al: Combretastatin A-4 phosphate as a tumor vascular-targeting agent: Early effects in tumor and normal tissues. Cancer Res 59:1626-1634, 1999
13. Beauregard DA, Thelwall PE, Chaplin DJ, et al: Magnetic resonance imaging and spectroscopy of combretastatin A4 prodrug-induced disruption of tumor perfusion and energetic status. Br J Cancer 77:1761-1767, 1998
14. Oxigene, Inc: Combretastatin A4 phosphate investigator's brochure. Boston, MA, Oxigene Inc, 1999
15. Miller AB, Hoogstraten B, Staquet M, et al: Reporting results of cancer treatment. Cancer 47:207-214, 1981
16. Stratford MRL, Dennis MF: Determination of combretastatin A-4 and its phosphate ester pro-drug in plasma by high-performance liquid chromatography. J Chromatogr B Biomed Sci Appl 721:77-85, 1999
17. Evelhoch JL: Key factors in the acquisition of contrast kinetic data for oncology. J Magn Reson Imaging 10:254-259, 1999
18. Tofts PS, Kermode AG: Measurement of the blood-brain barrier permeability and leakage space using dynamic MR imaging: 1. Fundamental concepts. Magn Reson Med 17:357-367, 1991
19. Tofts PS, Brix G, Buckley DL, et al: Estimating kinetic parameters from dynamic contrast-enhanced T(1)-weighted MRI of a diffusable tracer: Standardized quantities and symbols. J Magn Reson Imaging 10:223-232, 1999
20. Dowlati A, Robertson K, Cooney M, et al: A phase I pharmacokinetic and translational study of the novel vascular targeting agent combretastatin a-4 phosphate on a single-dose intravenous schedule in patients with advanced cancer. Cancer Res 62:3408-3416, 2002
21. Stark DB, Fletcher WS: Severe tumor pain associated with injection of vinblastine sulfate (NSC-49843). Cancer Chemother Rep 50:281-282, 1966
22. Kornek GV, Kornfehl H, Hejna M, et al: Acute tumor pain in patients with head and neck cancer treated with vinorelbine. J Natl Cancer Inst 88:1593, 1996
23. Mross K, Berdel WE, Feibig HH, et al: Clinical and pharmacologic phase I study of Cemadotin-HCL (LU103793), a novel antimitotic peptide, given as a 24-hour infusion in patients with advanced cancer: A study of the Arbeitsgemeinschaft Internistische Onkologie (AIO) Phase I Group and Arbeitsgruppe Pharmakologie in der Onkologie und Haematologie (APOH) Group of the German Cancer Society. Ann Oncol 9:1323-1330, 1998
24. Stevenson JP, Sun W, Gallagher M, et al: Phase I trial of the cryptophycin analogue LY355703 administered as an intravenous infusion on a day 1 and 8 schedule every 21 days. Clin Cancer Res 8:2524-2529, 2002
25. Rustin GJS, Galbraith SM, Taylor NJ, et al: Combretastatin A4 phosphate selectively targets vasculature in animal and human tumors. Clin Cancer Res 5:3732s, 1999 (suppl)
26. Belotti D, Vergani V, Drudis T, et al: The microtubule-affecting drug paclitaxel has antiangiogenic activity. Clin Cancer Res 2:1843-1849, 1996
27. Hu E, Ko R, Koda R, et al: Phase I toxicity and pharmacology study of trimethylcolchicinic acid in patients with advanced malignancies. Cancer Chemother Pharmacol 26:359-364, 1990
28. Platts SH, Falcone JC, Holton WT, et al: Alteration of microtubule polymerization modulates arteriolar vasomotor tone. Am J Physiol 277: H100-H106, 1999

29. Griggs J, Hesketh R, Smith GA, et al: Combretastatin-A4 disrupts neovascular development in non-neoplastic tissue. Br J Cancer 84:832-835, 2001

30. Ito H, Okafuji T, Suzuki T: Vitamin E prevents endothelial injury associated with cisplatin injection into the superior mesenteric artery of rats. Heart Vessels 10:178-184, 1995

31. Kohn S, Fradis M, Podoshin L, et al: Endothelial injury of capillaries in the stria vascularis of guinea pigs treated with cisplatin and gentamicin. Ultrastruct Pathol 21:289-299, 1997

32. Padhani AR, Husband JE: Dynamic contrast-enhanced MRI studies in oncology with an emphasis on quantification, validation and human studies. Clin Radiol 56:607-620, 2001

33. Donahue KM, Krouwer HG, Rand SD, et al: Utility of simultaneously acquired gradient-echo and spin-echo cerebral blood volume and morphology maps in brain tumor patients. Magn Reson Med 43:845-853, 2000

34. Brasch R, Turetschek K: MRI characterization of tumors and grading angiogenesis using macromolecular contrast media: Status report. Eur J Radiol 34:148-155, 2000

35. Davis DW, Mullani N, Hess KR, et al: Quantitative analysis of tumor vascular targeting: Effects of endostatin in a phase I clinical trial. Clin Cancer Res 7:3711s, 2001 (abstr 286)

36. Mundhenke C, Thomas JP, Neider R, et al: Endothelial cell kinetics in skin wounds and tumors of patients receiving endostatin. Proc Am Soc Clin Oncol 20:70a, 2001 (abstr 277)

37. Mayr NA, Yuh WT, Arnholt JC, et al: Pixel analysis of MR perfusion imaging in predicting radiation therapy outcome in cervical cancer. J Magn Reson Imaging 12:1027-1033, 2000

38. Galbraith SM, Lodge MA, Taylor NJ, et al: Reproducibility of dynamic contrast-enhanced MRI in human muscle and tumours: Comparison of quantitative and semi-quantitative analysis. NMR Biomed 15:132-142, 2002

39. Nelkin BD, Ball DW: Combretastatin A-4 and doxorubicin combination treatment is effective in a preclinical model of medullary thyroid carcinoma. Oncol Rep 8:157-160, 2001

40. Li L, Rojiani A, Siemann DW: Targeting the tumor vasculature with combretastatin A-4 disodium phosphate: Effects on radiation therapy. Int J Radiat Oncol Biol Phys 42:899-903, 1998

41. Grosios K, Loadman PM, Swaine DJ, et al: Combination chemotherapy with combretastatin A-4 phosphate and 5-fluorouracil in an experimental murine adenocarcinoma. Anticancer Res 20:229-233, 2000